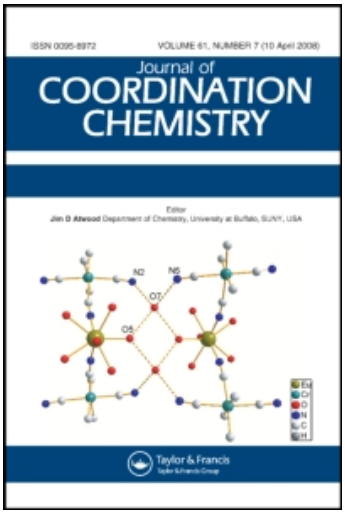

Journal of Coordination Chemistry
Publication details, including instructions for authors and subscription information:
http://www.informaworld.com/smpp/title~content=t713455674

Two new methylimidazole modified Hervé-sandwich-type polytungstoantimonates

Baowang Chen[a]; Weilin Chen[a]; Wenli Liu[a]; Yangguang Li[a]; Xinlong Wang[a]; Enbo Wang[a]
[a] Key Laboratory of Polyoxometalate Science of Ministry of Education, Department of Chemistry, Northeast Normal University, Changchun, Jilin 130024, P.R. China

First published on: 05 November 2010

To cite this Article Chen, Baowang , Chen, Weilin , Liu, Wenli , Li, Yangguang , Wang, Xinlong and Wang, Enbo(2011) 'Two new methylimidazole modified Hervé-sandwich-type polytungstoantimonates', Journal of Coordination Chemistry, 64: 1, 71 — 81, First published on: 05 November 2010 (iFirst)
To link to this Article: DOI: 10.1080/00958972.2010.527003
URL: http://dx.doi.org/10.1080/00958972.2010.527003

Journal of Coordination Chemistry
Vol. 64, No. 1, 10 January 2011, 71–81

Taylor & Francis
Taylor & Francis Group

Two new methylimidazole modified Hervé-sandwich-type polytungstoantimonates

BAOWANG CHEN, WEILIN CHEN, WENLI LIU, YANGGUANG LI, XINLONG WANG and ENBO WANG*

Key Laboratory of Polyoxometalate Science of Ministry of Education, Department of Chemistry, Northeast Normal University, Ren Min Street No. 5268, Changchun, Jilin 130024, P.R. China

(*Received 21 July 2010; in final form 7 September 2010*)

Two new polyoxometalate-based inorganic–organic hybrid compounds, $Na_9[\{Na(H_2O)_2\}_3\{M(C_4H_6N_2)\}_3(SbW_9O_{33})_2]\cdot 28H_2O$ (M = Co(**1**); M = Mn(**2**)), have been obtained by routine synthetic reactions in aqueous solutions and characterized by elemental analysis, IR, and thermogravimetric analyses. Single-crystal X-ray diffraction analyses reveal that **1** and **2** are isostructural and crystallize in the same space group $P\bar{1}$. The polyoxoanions in **1** and **2** are composed of two lacunary Keggin-type $[B\text{-}\alpha\text{-}SbW_9O_{33}]^{9-}$ building units, which are linked by three $[Na(H_2O)_2]^+$ cations and three $[M(C_4H_6N_2)]^{2+}$ (M = Co(**1**); M = Mn(**2**)) fragments, resulting in sandwich-type structures. Furthermore, the sandwich-type polyoxoanions are connected into 3-D frameworks *via* Na^+ and extensive hydrogen-bonding interactions along the *a*-axis. Electrochemical and photochemical catalysis activities of **1** and **2** have also been investigated.

Keywords: Heteropolyoxotungstates; Sandwich-type; Tungstoantimonate; Methylimidazole

1. Introduction

Polyoxometalates (POMs) have attracted extensive attention owing to their interesting structural diversities and potential applications in catalysis, medicine, magnetism, and materials science [1]. Sandwich-type polyoxoanions based on trivacant Keggin $[XW_9O_{33\text{ or }34}]^{n-}$ building units represent an important subclass [2]. A great number of sandwich-type polyoxoanions have been continuously reported with most belonging to the well-known Weakley- [3], Hervé- [4], Krebs- [5], and Knoth- [6] type sandwich structures.

Hervé-type sandwich structure was first reported by Robert *et al*. in 1982 [7]. Subsequently, synthetic chemists obtained a series of transition metal substituted compounds, $[M_3(H_2O)_3(XW_9O_{33})_2]^{n-}$ ($X = As^{III}$, Sb^{III}, Bi^{III}, Se^{III}, and Te^{III}; $M = Mn^{2+}$, Ni^{2+}, Co^{2+}, Cu^{2+}, and Zn^{2+}) [8]. Generally, the Hervé-type polyoxoanion consists of two $[B\text{-}\alpha\text{-}XW_9O_{33}]^{9-}$ moieties linked by three equivalent transition metals resulting in a

*Corresponding author. Email: wangeb889@nenu.edu.cn; wangenbo@public.cc.jl.cn

ISSN 0095-8972 print/ISSN 1029-0389 online
DOI: 10.1080/00958972.2010.527003

sandwich-type structure with idealized D_{3h} symmetry. Each transition metal in the belt coordinates to four terminal oxygens from four WO_6 groups of two different [*B*-α-$XW_9O_{33}]^{9-}$ units and an oxygen from water, representing square-pyramidal geometry. Coordination water molecules in Hervé-type sandwich polyoxoanions are inclined to substitute with organic molecules [9], which have presented significant nonlinear optical properties and liquid-crystal behaviors in phase transfer systems [10]. Here we report two new methylimidazole modified Hervé-type polytungstoantimonates, $Na_9[\{Na(H_2O)_2\}_3\{M(C_4H_6N_2)\}_3(B\text{-}\alpha\text{-}SbW_9O_{33})_2]\cdot 28H_2O$ (M = Co(**1**); M = Mn(**2**)). The polyoxoanions in **1** and **2** are composed of the Hervé-type sandwich polyoxoanions, which are modified by methylimidazole. The sandwich-type polyoxoanions are further connected into 3-D frameworks *via* Na^+ and extensive hydrogen bonding. Electrochemical and photo-catalytic properties of **1** and **2** have been studied.

2. Experimental

2.1. *General methods and materials*

All chemicals were commercially purchased and used without purification. Elemental analyses (C, H, and N) were performed on a Perkin-Elmer 2400 CHN elemental analyzer. Na, Co, Mn, Sb, and W were performed by a Leaman inductively coupled plasma (ICP) spectrometer; IR spectra were recorded from 400 to 4000 cm^{-1} on an Alpha Centaurt FT-IR Spectrophotometer with pressed KBr pellets. UV-Vis absorption spectra were obtained using a 752 PC UV-Vis spectrophotometer. Thermal stabilities of **1** and **2** were determined by TG analysis on a Perkin-Elmer TGA7 instrument in flowing N_2 with a heating rate of 10°C min^{-1}. All electrochemical experiments were recorded on a CHI 600 electrochemical workstation at room temperature. A conventional three-electrode system is used. The working electrode is glassy carbon, an SCE is employed as the reference electrode and platinum wire as a counter electrode. The media for the electrochemical studies are 0.2 mol L^{-1} H_2SO_4/$NaSO_4$ (pH = 3.00) solutions. Thrice-distilled water is used throughout the experiments. A pHS-25B type pH meter was used for pH measurements.

2.2. *Photocatalysis*

Aqueous solution was prepared by adding the sample (0.0237 g for **1** or 0.0236 g for **2**) to a 200 mL solution of rhodamine-B (RhB) dye (2×10^{-5} mol L^{-1}). Prior to irradiation, the mixed solution was magnetically stirred in the dark for 20 min to ensure equilibrium of the working solution. The solution was exposed to UV irradiation from a 125 W Hg lamp. At given time intervals, 3 mL of samples was taken from the beaker. The solution was used for UV-Vis absorption analysis.

2.3. *Syntheses*

2.3.1. Synthesis of 1. $SbCl_3$ (0.21 g, 0.90 mmol) dissolved in 1 mL of 6 mol L^{-1} HCl was added to a solution of $Na_2WO_4\cdot 2H_2O$ (2.97 g, 9 mmol) in 30 mL of deionized

water, and the mixture was heated to 80°C for about 15 min. Then 5 mL of 0.25 mol L^{-1} $Co(CH_3COO)_2 \cdot 4H_2O$ solution and 0.5 mL methylimidazole were added to the clear solution successively, and the pH of the mixture was adjusted to 7.45 at room temperature by addition of 1 mol L^{-1} HCl. The solution was then heated to boiling for 3 h. After cooling to room temperature, the solution was filtered and the filtrate was slowly evaporated at room temperature for 7 days, resulting in the blue block crystalline product (51% yield based on Co). Calcd for **1** (%): C, 2.43; H, 1.47; N, 1.42; Co, 2.99; Na, 4.66; Sb, 4.11; W, 55.90. Found: C, 2.37; H, 1.58; N, 1.48; Co, 3.12; Na, 4.75; Sb, 4.02; W, 56.12. IR (KBr pellets): 3422(br), 2105(br), 1628(vs), 1536(s), 1416(w), 1288(w), 1237(s), 1098(s), 937(m), 869(m), 719(m).

2.3.2. Synthesis of 2. Preparation of **2** was similar to that of **1** except that $Mn(CH_3COO)_2 \cdot 4H_2O$ was used instead of $Co(CH_3COO)_2 \cdot 4H_2O$ (49% yield based on Mn). Calcd for **2** (%): C, 2.44; H, 1.47; N, 1.42; Mn, 2.79; Na, 4.67; Sb, 4.12; W, 56.01. Found: C, 2.37; H, 1.38; N, 1.46; O, Mn, 2.85; Na, 4.79; Sb, 4.01; W, 55.82. IR (KBr pellets): 3441(br), 2065(br), 1628(vs), 1537(w), 1288(w), 1240(s), 1114(w), 1092(w), 938(s), 864(s), 719(s).

2.4. *X-ray crystallography*

Single crystal X-ray data for compounds were collected on a Rigaku R-AXISRAPID IP diffractometer equipped with a normal focus 18 kW sealed tube X-ray source (Mo-Kα radiation, $\lambda = 0.71073$ Å) operating at 50 kV and 200 mA. The structures were solved by direct methods and refined by full-matrix least-squares on F^2 using *SHELX-97* software [11]. The empirical absorption correction was applied. As usual for POMs, the crystal shows large disorder for counterions and water molecules [12]. Therefore, elemental analysis is instrumental to determine the correct sodium content. The exact formula was determined by elemental analysis and TG analysis. Further details of the X-ray structure analysis are given in table 1; selected bond lengths and angles for **1** and **2** are given in table S1.

3. Results and discussion

3.1. *Syntheses*

The Hervé-type sandwich POMs with Sb^{III} as the hetero atom have been known for a long time. The presence of the lone pair of electrons in Sb^{III} precludes closing of the Keggin unit, resulting in many novel tungstoantimonates with unexpected structures to be obtained [13]. The compounds were prepared by conventional synthetic methods. In our experiments, we do not use the lacunary Keggin precursor $[B\text{-}SbW_9O_{33}]^{9-}$ or cryptate precursor $[NaSb_9W_{21}O_{86}]^{9-}$, but directly employ simple raw materials of $SbCl_3$, Na_2WO_4, transition-metal ions (Co^{2+}, Mn^{2+}), and methylimidazole. The pH values are crucial for syntheses of **1** and **2**; no compounds were obtained when pH values are more than 8.0 or less than 7.0. The syntheses need longer reaction time ($t > 2$ h) and higher reaction temperature ($T > 80$°C) to form enough $[B\text{-}\alpha\text{-}SbW_9O_{33}]^{9-}$

Table 1. Crystal data and structure refinement of **1** and **2**.

Compounds	**1**	**2**
Empirical formula	$C_{12}H_{86}Co_3N_6Na_{12}O_{100}Sb_2W_{18}$	$C_{12}H_{86}Mn_3N_6Na_{12}O_{100}Sb_2W_{18}$
Formula weight	5920.34	5908.37
Temperature (K)	150(2)	150(2)
Wavelength (Å)	0.71073	0.71073
Crystal system	Triclinic	Triclinic
Space group	$P\bar{1}$	$P\bar{1}$
Unit cell dimensions (Å, °)		
a	13.560(3)	13.562(3)
b	19.104(4)	19.107(4)
c	24.933(5)	24.917(5)
α	75.70(3)	75.66(3)
β	85.68(3)	85.80(3)
γ	74.04(3)	74.04(3)
Volume (Å^3), Z	6017(2), 2	6014(2), 2
Calculated density (Mg m^{-3})	3.268	3.263
Absorption coefficient, μ (mm^{-1})	18.115	18.025
$F(000)$	5294	5282
Data/restraints/parameters	19,813/297/1389	20,545/650/1301
Goodness-of-fit on F^2	1.051	1.018
Final R indices [$I > 2\sigma(I)$]	$R_1 = 0.0519$, $wR_2 = 0.1254$	$R_1 = 0.0754$, $wR_2 = 0.1923$

$R_1 = ||F_o| - |F_c||/|F_o|$; $wR_2 = [w(F_o^2 - F_c^2)^2]/[w(F_o^2)^2]^{1/2}$.

building blocks. Methylimidazole with low concentration cannot substitute coordinated water attached to the magnetic metal cluster of sandwich-type POMs in aqueous solution because of coordination competition between water and organic ligand. By parallel experiments, we found that no desired compounds were obtained when methylimidazole added is less than 0.30 mL. Hence reaction time, temperature, and ionic strength are key factors to obtain crystals in higher yield.

3.2. *Structure description*

Single-crystal X-ray diffraction analyses reveal that **1** and **2** are isostructural; the unit cell dimensions and volumes are only slightly changed, so here we discuss the structure of **1**. Compound **1** is composed of a sandwich-type anionic moiety $[\{Na(H_2O)_2\}_3\{Co(C_4H_6N_2)\}_3(B\text{-}\alpha\text{-}SbW_9O_{33})_2]^{9-}$ (**1**a), nine Na^+ cations and 28 lattice water molecules (figure 1). The polyanion **1**a consists of two lacunary $[B\text{-}\alpha\text{-}SbW_9O_{33}]^{9-}$ building units, which are connected by a methylimidazole modified cluster $[\{Na(H_2O)_2\}_3\{Co(C_4H_6N_2)\}_3]^{9+}$ (figure 1b). In the center of each $[B\text{-}\alpha\text{-}SbW_9O_{33}]^{9-}$ unit containing three corner sharing W_3O_{13} triads, the Sb(III) forms a SbO_3 trigonal pyramid with Sb–O bond lengths of 1.969(9)–1.997(1) Å and the lone-pair electrons are directed toward the opening of the unit (table S1). Each Co has square-pyramidal geometry, coordinated with four terminal oxygens from four WO_6 groups of two different $[B\text{-}\alpha\text{-}SbW_9O_{33}]^{9-}$ units with Co–O bond lengths of 2.004(1)–2.050(1) Å and a nitrogen from methylimidazole with Co–N bond lengths ranging from 2.016(1) to 2.053(2) Å. The space between the three transition metal ions is occupied by three sodium ions leading to a central belt of six metals alternating in sandwiching position

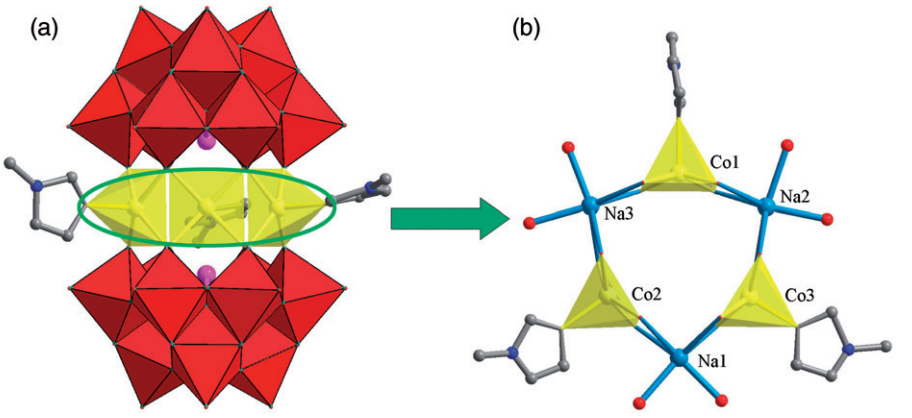

Figure 1. (a) Polyhedral and ball-and-stick representation of **1**a. Color code: W (red octahedra), Co (yellow square-pyramid), Sb (purple), O (red), N (blue), and C (gray). (b) Coordination environment of the hexanuclear cluster in the central belt. Color code: Co (yellow square-pyramid), Na (light blue), O (red), N (blue), and C (gray).

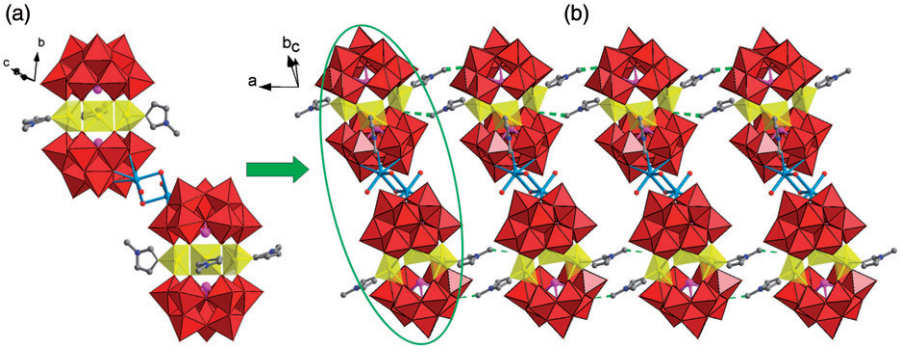

Figure 2. (a) The sandwich dimer unit in **1**. Color code: W (red octahedra), Co (yellow square-pyramid), Sb (purple), Na (light blue), O (red), N (blue), and C (gray). (b) View of 1-D infinite supramolecular chain of **1** along the *c*-axis. Color code: W (red octahedra), Co (yellow square-pyramid), Sb (purple), Na (light blue), O (red), N (blue), and C (gray).

(figure 1b). Each sodium is coordinated by four oxygens from two $[B\text{-}\alpha\text{-}SbW_9O_{33}]^{9-}$ units and two terminal water molecules to form a $\{NaO_6\}$ octahedron. The bond lengths of $Na–O_{POM}$ are in the range 2.410(1)–2.536(1) Å, while the distances of $Na–O_W$ range from 2.386(2) to 2.47(2) Å (table S2).

Adjacent sandwich-type polyanions are connected by a binuclear $[Na_2(H_2O)_4]^{2+}$ forming a sandwich dimer (figure 2a). Neighboring sandwich dimers are connected to a 1-D infinite supramolecular chain through extensive hydrogen-bonding interactions between organic groups and oxygen of the sandwich-type POMs (C10···O22; 3.178(4) Å; C12···O46, 3.059(5) Å) along the *c*-axis (figure 2b). Furthermore, The 1-D chains are connected into 3-D frameworks *via* Na^+ and extensive $O_W \cdots O_{POMs}$ hydrogen-bonding interactions (Ow7…O48, 2.886(4) Å; Ow7···O5, 2.706(3) Å; Ow12…O48, 2.838(5) Å; Ow12···O17, 2.831(2) Å; Ow11···O51, 2.828(3) Å; Ow13···O50, 2.822(4) Å) along the *a*-axis (figure 3).

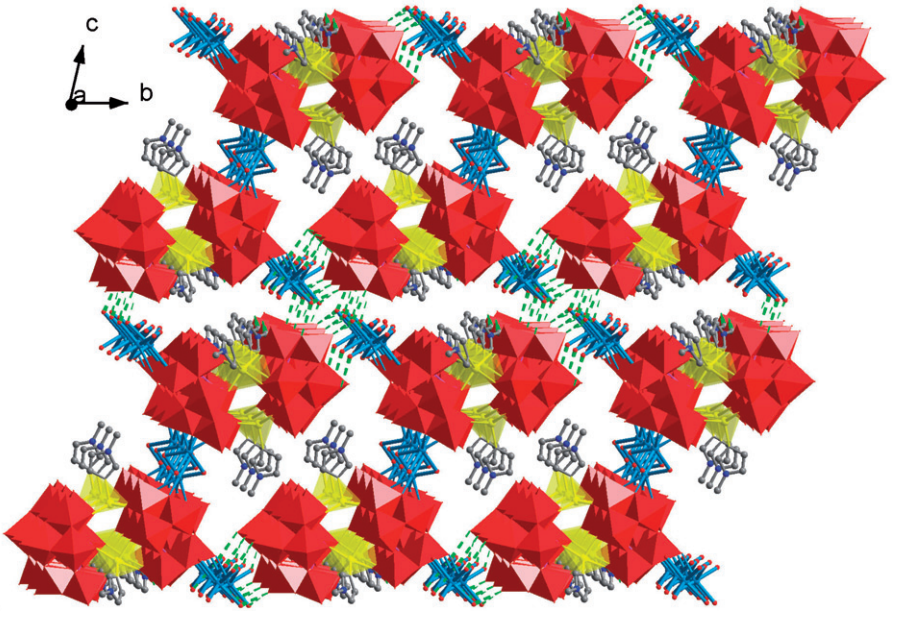

Figure 3. View of 3-D supramolecular framework of **1** along the *a*-axis. W (red octahedra), Sb (purple), Co (yellow square-pyramid), Na (light blue), O (red), N (blue), and C (gray).

3.3. *IR spectrum*

In the IR spectrum of **1** (figure S1), the broad peak at 3422 cm^{-1} is assigned to water [14]. Peaks at 1628, 1536, 1416, 1288, and 1237 cm^{-1} correspond to ν(C=C) and ν(C=N) [15]; characteristic peaks at 937, 869, and 719 cm^{-1} are attributed to vibrations of the polyanions [16]. The peak at 1089 cm^{-1} is attributed to ν(C–H) in the imidazole ring [17]. In the IR spectrum of **2** (figure S2), the broad peak at 3441 cm^{-1} is assigned to water [14]. Peaks at 1628, 1537, 1288, and 1240 cm^{-1} correspond to ν(C=C) and ν(C=N) [15], while those at 1114 and 1092 cm^{-1} are attributed to ν(C–H) in the imidazole ring [16]. Characteristic peaks at 938, 864, and 719 cm^{-1} are attributed to vibrations of the polyanions [17].

3.4. *Cyclic voltammogram*

- Electrochemical properties of **1** and **2** were carried out in pH = 3 (0.2 mol L^{-1} H_2SO_4+Na_2SO_4) buffer solutions at the scan rate of 100 mV s^{-1}. Figure 4 shows the cyclic voltammogram (CV) of **1**. In the potential range from −0.7 to −1.3 V, two reversible redox peaks appear and the mean peak potentials $E_{1/2} = (E_{pa} + E_{pc})/2$ are −1.122 V (I–I′) and −0.974V (II–II′) (*vs.* SCE), respectively. The two reversible peaks I–I′ and II–II′ correspond to redox of the W^{VI} in the polyoxoanion framework and the domain where the waves are located is similar to other tungsten-containing POMs [18]. The CV of **2** exhibits two redox peaks with mean peak potential values at −1.089 and −0.955 V (*vs.* SCE) (figure 5), very similar to that of **1** in the negative potential domain and they are also ascribed to the redox process of the W centers. In the

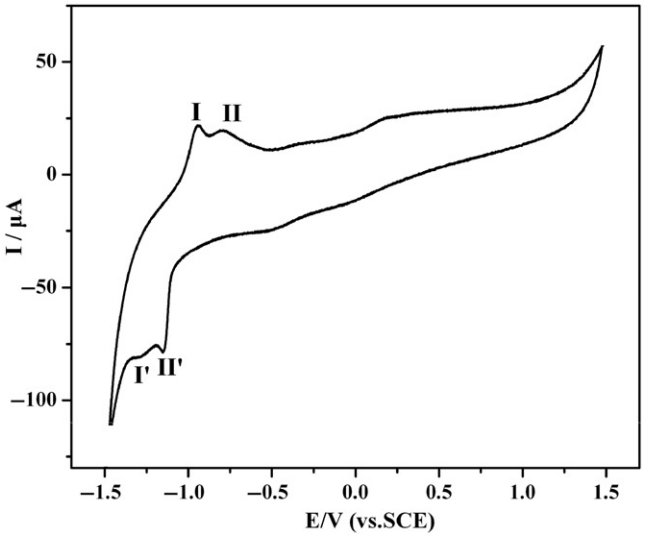

Figure 4. CV curve of **1** in pH = 3.00 solution (0.2 mol L^{-1} H_2SO_4+Na_2SO_4) at the scan rate of 100 mV s^{-1}.

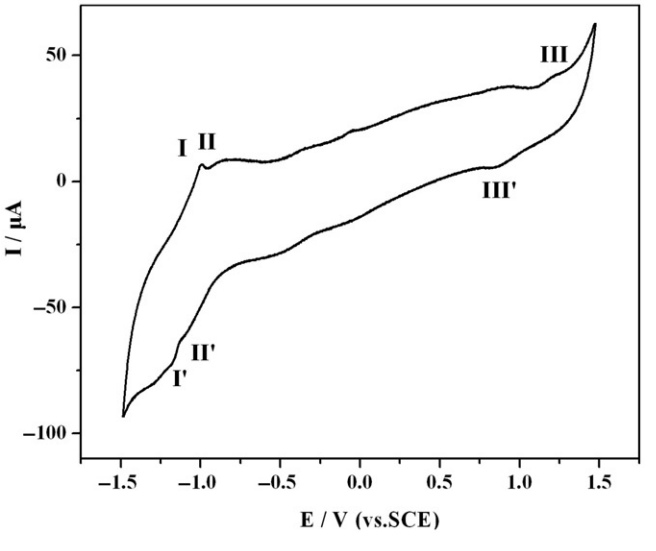

Figure 5. CV curve of **2** in pH = 3.00 solution (0.2 mol L^{-1} H_2SO_4+Na_2SO_4) at scan rate of 100 mV s^{-1}.

positive potential domain, the third pair of peaks (III–III′) appear at positive potentials of 1.210 V for oxidation and 0.864 V for reduction and this pair of redox peaks is attributed to redox of the Mn-centered reaction [19].

3.5. *Photocatalytic properties*

In order to examine catalytic properties of the compounds, photocatalytic degradations of RhB were investigated. The photocatalytic activity of **1** is taken for example and **2** is

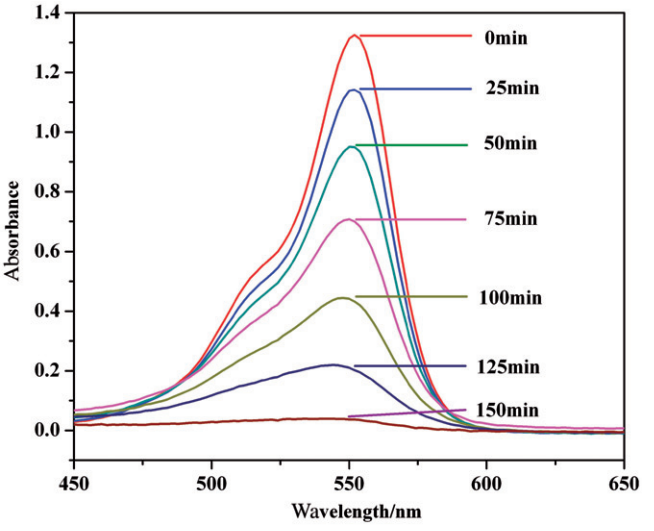

Figure 6. The UV-Vis absorption spectrum changes of RhB for different times recorded for solution including 2×10^{-5} mol L^{-1} RhB and 2×10^{-5} mol L^{-1} **1.**

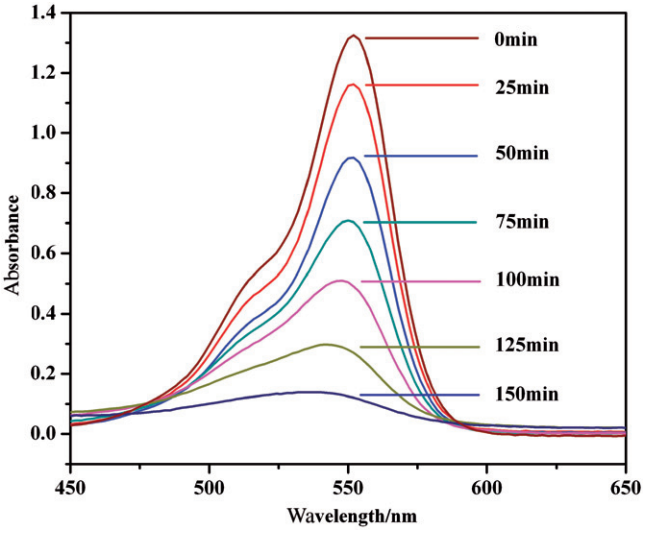

Figure 7. The UV-Vis absorption spectral changes of RhB for different times recorded at the solution including 2×10^{-5} mol L^{-1} RhB and 2×10^{-5} mol L^{-1} **2**.

discussed in brief. Figure 6 is the UV-Vis absorption spectra for different times recorded for 2×10^{-5} mol L^{-1} RhB and 2×10^{-5} mol L^{-1} **1**. The UV-Vis absorption peaks of RhB decrease under the irradiations; after 2.5 h, the absorption peaks were very weak, indicating that **1** exhibits photocatalysis [20]. Compound **2** also reveals excellent photocatalytic activity (figure 7). In figure 8, we plot conversion of RhB (K) *versus* reaction time (t) of **1** and **2**. The conversion of RhB (K) can be expressed

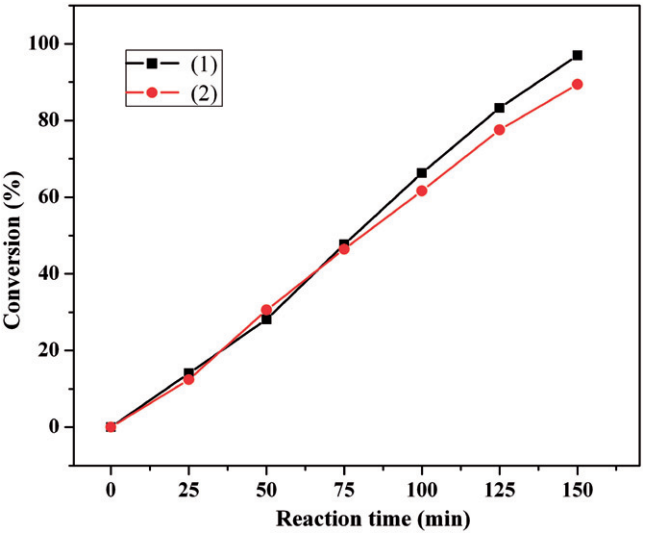

Figure 8. Plot of the conversions of RhB *vs.* reaction time for the photocatalyzed solutions of **1** and **2**.

as $K=(I_0-I_t)/I_0$, where I_0 represents the UV-Vis intensity of RhB at the original reaction ($t=0$) and I_t is the UV-Vis absorption intensity at a certain time t [21]. The results show that the conversion of RhB using **1** as the photocatalyst is 96.98% during 2.5 h irradiation, while that of **2** is 89.39%. Recently, Zhao *et al.* [22] investigated the photocatalytic degradation of RhB by Keggin POM $H_4SiW_{12}O_{40}$. Compared with the catalytic effect of simple pure-inorganic POM, inorganic–organic hybrid compounds **1** and **2** show better catalytic activities.

3.6. *Thermogravimetric analyses*

The thermogravimetric (TG curve of **1** exhibits three steps of weight loss (figure S3). The first of 10.46% from 22°C to 336°C corresponds to loss of all lattice and coordinated water, in accord with the calculated value of 10.35%. The second weight loss is 2.73% from 336°C to 377°C, assigned to loss of two methylimidazoles (Calcd 2.77%). The last weight loss of 1.43% is attributed to loss of one methylimidazole from 377°C–504°C (Calcd 1.39%). The TG curve of **2** also shows three steps of weight loss (figure S4). The first of 10.33% from 24°C to 337°C corresponds to loss of all lattice and coordinated water (Calcd 10.37%). The second weight loss (2.73%) at 337°C–373°C is attributed to loss of two methylimidazoles (Calcd 2.78%) and the last of 1.36% is attributed to loss of one methylimidazole (373°C–507°C, Calcd 1.39%).

4. Conclusion

Two new M_3-substituted POM-based inorganic–organic hybrid compounds were synthesized. Compounds **1** and **2** enrich the diversity of sandwich-type POMs and

provide an effective way for making inorganic–organic composite transition metal substituted POMs. Further research on the inorganic–organic hybrid compounds of M_3-substituted POMs is currently underway.

Supplementary material

Crystal data with CCDC reference numbers: **1**: 783119; **2**: 783120 have been deposited with the Cambridge Crystallographic Center; copy of this information may be obtained free of charge from The Director, CCDC, 12 Union Road, Cambridge, CB2 IEZ, UK (Fax: +44123336033; E-mail: deposit@ccdc.cam.ac.uk). X-ray crystallographic files in CIF format; TG curves; IR spectra; selected bond lengths (Å) and angles (°) for **1** and **2**, and the bond lengths (Å) of Na–O_W and Na–O_{POM} for **1** are available online.

Acknowledgments

This study was supported by the National Natural Science Foundation of China (no. 20701005), National Natural Science Foundation of China (no. 20701006), Science and Technology Creation Foundation of Northeast Normal University (NENU-STC07009), and the Testing Foundation of Northeast Normal University.

References

[1] (a) M.I. Khan, R.C. Haushalter, C.J. O'Connor, C. Tao, J. Zubieta. *Chem. Mater*., **7**, 593 (1995); (b) O.M. Yaghi, M. O'Keeffe, N.W. Ockwig, H.K. Chae, M. Eddaoudi, J. Kim. *Nature*, **423**, 705 (2003); (c) C.L. Hill, C.M. Prosser-Mccartha. *Coord. Chem. Rev*., **143**, 407 (1995); (d) M.T. Pope, A. Müller. *Angew. Chem. Int. Ed. Engl*., **30**, 34 (1991).

[2] (a) X. Zhang, T.M. Anderson, Q. Chen, C.L. Hill. *Inorg. Chem*., **40**, 418 (2001); (b) R.G. Finke, M. Droege, J.R. Hutchinson, O. Gansow. *J. Am. Chem. Soc*., **103**, 1587 (1981); (c) Z.M. Zhang, E.B. Wang, Y.F. Qi, Y.G. Li, B.D. Mao, Z.M. Su. *Cryst. Growth Des*., **7**, 1305 (2007).

[3] (a) T.J.R. Weakley, H.T. Evans, J.S. Showell, G.F. Tourné, C.M. Tourné. *J. Chem. Soc., Chem. Commun*., 139 (1973); (b) T.J.R. Weakley, R.G. Finke. *Inorg. Chem*., **29**, 1235 (1990); (c) Z. Luo, P. Kögerler, R. Cao. C.L. Hill. *Inorg. Chem*., **48**, 7812 (2009); (d) U. Kortz, S. Isber, M.H. Dickman, D. Ravot. *Inorg. Chem*., **39**, 2915 (2000).

[4] (a) Y.H. Liu, P.T. Ma, J.P. Wang. *J. Coord. Chem*., **61**, 936 (2008); (b) D. Volkmer, B. Bredenkötter, J. Tellenbröker, P. Kögerler, D.G. Kurth, P. Lehmann, H. Schnablegger, D. Schwahn, M. Piepenbrink, B. Krebs. *J. Am. Chem. Soc*., **124**, 10489 (2002).

[5] (a) E.M. Limanski, D. Drewes, E. Droste, R. Bohner, B. Krebs. *J. Mol. Struct*., **656**, 17 (2003); (b) D. Drewes, E.M. Limanski, M. Piepenbrink, B. Krebs. *Z. Anorg. Allg. Chem*., **630**, 58 (2004); (c) I. Loose, E. Droste, M. Bösing, H. Pohlmann, M.H. Dickman, C. Rosu, M.T. Pope, B. Krebs. *Inorg. Chem*., **38**, 2688 (1999); (d) U. Kortz, M.G. Savelieff, B.S. Bassil, B. Keita, L. Nadjo. *Inorg. Chem*., **41**, 783 (2002).

[6] (a) W.H. Knoth, P.J. Domaille, R.D. Farlee. *Organometallics*, **4**, 62 (1985); (b) R.G. Finke, B. Rapko, T.J.R. Weakley. *Inorg. Chem*., **28**, 1573 (1989); (c) F.B. Xin, M.T. Pope. *J. Am. Chem. Soc*., **118**, 7731 (1996).

[7] F. Robert, M. Leyrie, G. Hervé. *Acta Crystallogr., Sect. B*, **38**, 358 (1982).

[8] (a) P. Mialane, J. Marrot, E. Rivière, J. Nebout, G. Hervé. *Inorg. Chem*., **40**, 44 (2001); (b) M. Bösing, A. Nöh, I. Loose, B. Krebs. *J. Am. Chem. Soc*., **120**, 7252 (1998).

[9] (a) R.R. Cui, H.L. Wang, X.Y. Yang, S.H. Ren, H.M. Hu, F. Fu, J.W. Wang, G.L. Xue. *Chin. J. Chem.*, **25**, 176 (2007); (b) H.L. Wang, G.L. Xue, J.W. Wang, D.Q. Wang, J. Li, Q.Z. Shi. *Acta Chim. Sinica*, **61**, 1839 (2003) (in Chinese); (c) H. Liu, C. Qin, Y.G. Wei, L. Xu, G.G. Gao, F.Y. Li, X.S. Qu. *Inorg. Chem.*, **47**, 4166 (2008); (d) H. Liu, L. Xu, Y.F. Qiu, W.J. An, Y.N. Jin, B.B. Xu. *Chem. J. Chin. Univ.*, **27**, 1409 (2006).
[10] (a) L.H. Bi, E.B. Wang, J. Peng, R.D. Huang, L. Xu, C.W. Hu. *Inorg. Chem.*, **39**, 671 (2000); (b) L.H. Bi, R.D. Huang, J. Peng, E.B. Wang, Y.H. Wang, C.W. Hu. *J. Chem. Soc., Dalton Trans.*, 121 (2001); (c) J. Peng, E.B. Wang, Y.S. Zhou. *J. Chem. Soc., Dalton Trans.*, 3865 (1998).
[11] (a) G.M. Sheldrick. *SHELX 97, Program for Crystal Structures Refinement*, University of Göttingen, Germany (1997); (b) G.M. Sheldrick. *SHELX 97, Program for Crystal Structures Solution*, University of Göttingen, Germany (1997).
[12] (a) U. Kortz, N.K. Al-Kassem, M.G. Savelieff, N.A. Al Kadi, M. Sadakane. *Inorg. Chem.*, **40**, 4742 (2001); (b) R.R. Cui, H.L. Wang, X.Y. Yang, S.H. Ren, H.M. Hu, F. Fu, J.W. Wang, G.L. Xue. *Chin. J. Chem.*, **25**, 176 (2007).
[13] (a) J. Fischer, L. Ricard, R. Weiss. *J. Am. Chem. Soc.*, **98**, 3050 (1976); (b) M. Bösing, I. Loose, H. Pohlmann, B. Krebs. *Chem. Eur. J.*, **3**, 1232 (1997); (c) J.P. Wang, P.T. Ma, J. Li, H.Y. Niu, J.Y. Niu. *Chem. Asian J.*, **3**, 822 (2008).
[14] (a) J.P. Wang, Y.Q. Feng, P.T. Ma, J.Y. Niu. *J. Coord. Chem.*, **62**, 1895 (2009); (b) J.P. Wang, J.J. Wang, P.T. Ma, J.Y. Niu. *J. Coord. Chem.*, **62**, 2641 (2009).
[15] L. Han, P.P. Zhang, H.S. Liu, H.J. Pang, Y. Chen, J. Peng. *J. Cluster Sci.*, **21**, 81 (2010).
[16] (a) L.H. Bi, B. Li, L.X. Wu, Y.Y. Bao. *Inorg. Chim. Acta*, **362**, 3309 (2009); (b) M. Bösing, I. Loose, H. Pohlmann, B. Krebs. *Chem. Eur. J.*, **3**, 1232 (1997).
[17] D.S. Jacob, S. Makhluf, I. Brukental, R. Lavi, L.A. Solovyov, I. Felner, I. Nowik, R. Persky, H.E. Gottlieb, A. Gedanken. *Eur. J. Inorg. Chem.*, 2669 (2005).
[18] (a) I.M. Mbomekalle, B. Keita, M. Nierlich, U. Kortz, P. Berthet, L. Nadjo. *Inorg. Chem.*, **42**, 5143 (2003); (b) B. Keita, I.M. Mbomekalle, Y.W. Lu, L. Nadjo, P. Berthet, T.M. Anderson, C.L. Hill. *Eur. J. Inorg. Chem.*, 3462 (2004); (c) B. Keita, I.M. Mbomekalle, L. Nadjo, R. Contant. *Electrochem. Commun.*, **3**, 267 (2001).
[19] (a) Z.M. Zhang, E.B. Wang, W.L. Chen, H.Q. Tan. *Aust. J. Chem.*, **60**, 284 (2007); (b) X.Y. Zhang, C.J. O'Connor, G.B. Jameson, M.T. Pope. *Inorg. Chem.*, **35**, 30 (1996); (c) J.F. Liu, F. Ortega, M.T. Pope. *J. Chem. Soc., Dalton Trans.*, 1901 (1992).
[20] (a) H.B. Fu, C.S. Pan, W.Q. Yao, Y.F. Zhu. *J. Phys. Chem. B*, **109**, 22432 (2005); (b) M.C. Yin, Z.S. Li, J.H. Kou, Z.G. Zou. *Environ. Sci. Technol.*, **43**, 8361 (2009).
[21] (a) L.L. Li, Y. Chu, Y. Liu, L.H. Dong. *J. Phys. Chem. C*, **111**, 2123 (2007); (b) W.L. Chen, B.W. Chen, H.Q. Tan, Y.G. Li, Y.H. Wang, E.B. Wang. *J. Solid State Chem.*, **183**, 310 (2010).
[22] C.C. Chen, W. Zhao, P.X. Lei, J.C. Zhao, N. Serpone. *Chem. Eur. J.*, **10**, 1956 (2004).